Synthesis, Characterization and Electronic Properties of an Endohedral Plumbaspherene $[Au@Pb_{12}]^{3-}$

Lei-Jiao Li,[a, †] Fu-Xing Pan,[a, b,†] Feng-Yu Li, [c] Zhong-Fang Chen,[c]* and Zhong-Ming Sun,[a, d]*

[a] State Key Laboratory of Rare Earth Resource Utilization, Changchun Institute of Applied Chemistry, Chinese Academy of Sciences, 5625 Renmin Street, Changchun, Jilin 130022, China.

[b] Key Laboratory of Nonferrous Metals Chemistry and Resources Utilization of Gansu Province and State Key Laboratory of Applied Organic Chemistry, College of Chemistry and Chemical Engineering, Lanzhou University, Lanzhou 730000, PR China.

[c] Department of Chemistry, Institute for Functional Nanomaterials, University of Puerto Rico, San Juan, PR 00931, USA.

[d] State Key Laboratory of Coordination Chemistry, School of Chemistry and Chemical Engineering, Nanjing University, Nanjing 210023, P. R. China.

[†]These authors contributed equally to this work.

Content:

1. Synthesis of $[K([2.2.2]crypt)]_3[Au@Pb_{12}]\cdot 2py$
2. X-ray crystal structure determination
3. ^{207}Pb NMR spectrum
4. Computational details
5. References

1. Synthesis of $[K([2.2.2]crypt)]_3[Au@Pb_{12}]\cdot 2Py$

All manipulations and reactions were performed under a nitrogen atmosphere using standard Schlenk or glovebox techniques. Ethylenediamine (en) (Aldrich, 99%) was freshly distilled by CaH_2 prior to use. Toluene (tol) (Aldrich, 99.8%) was distilled from sodium/benzophenone under dinitrogen and stored under dinitrogen. K (Aldrich, 99%), Na (Aldrich, 99.7%), Pb (Aldrich, 99.9%), CaH_2 (Aldrich, 99.99%), and benzophenone (Aldrich, 99.5%) were used as received. [2.2.2]crypt (4,7,13,16,21,24-Hexaoxa-1,10-diazabicyclo[8.8.8]hexacosane, TCI, 98%,) were dried in a vacuum for 1 d. K_4Pb_9 and $Au(PPh_3)Ph$ were prepared according to literatures, respectively. [1-2]

Synthesis of $[K([2.2.2]crypt)]_3[Au@Pb_{12}]\cdot 2Py$: In a 10 mL vial, 202 mg (0.10 mmol) of K_4Pb_9 and 100 mg (0.27 mmol) of [2.2.2]crypt were dissolved in pyridine (2 mL). In a second vial, 50 mg (0.09 mmol) $Au(PPh_3)Ph$ was dissolved in 0.5 mL toluene. The toluene solution was added to ethylenediamine solution dropwise while stirring vigorously. After 4h at room temperature, the resulting blcak solution was filtered through glass wool and transferred to a test tube, then carefully layered by toluene (3 mL). After 3 days, dark red crystals of

$[K([2.2.2]crypt)]_3[Au@Pb_{12}]\cdot 2Py$ (23% yield based on Au) appeared on the interface of the tube wall.

2. X-ray crystal structure determinations

Crystallographic data were collected at 298 K on a Bruker Apex II CCD diffractometer with graphite-monochromated Mo Kα radiation (λ = 0.71073 Å). Data processing was accomplished with the SAINT program.[3] The structures were solved by direct methods and refined on F^2 by full-matrix least squares using SHELXTL[4]. The CCDC number of $[K([2.2.2]crypt)]_3[Au@Pb_{12}]\cdot 2Py$ is 1492938. These data can be obtained free of charge from The Cambridge Crystallographic Data Centre via www.ccdc.cam.ac.uk/data_request/cif.

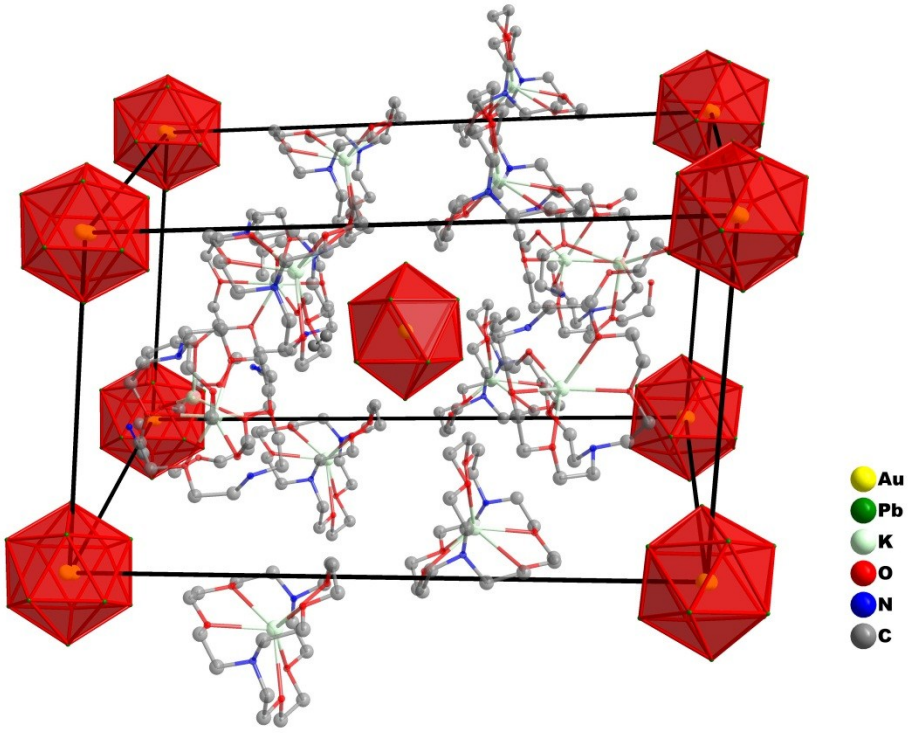

Figure S1. Unit cell of $[K([2.2.2]crypt)]_3[Au@Pb_{12}]\cdot 2Py$. Hydrogen atoms have been omitted for clarity.

Table S1. X-ray measurement and structure solutions of $[K([2.2.2]crypt)]_3[Au@Pb_{12}]\cdot 2Py$.

Compound	$C_{64}H_{118}N_8O_{36}K_3AuPb_{12}$
Formula weight	4376.3155
Crystal system	triclinic
Space group	*P-1*
a /Å	14.4831(14)
b /Å	14.7999
c /Å	27.187(3)
a /°	95.424
β	93.193(2)
γ	109.314(2)
V	5451.7(9)
Z	2
ρ_{calc} /g·cm^{-3}	2.479

$\mu(Mo_{K\alpha})$ /mm^{-1}	19.956
2Θ range /°	1.68-52.18
Reflections collected / unique	56398 / 19229
Data / restraints / parameters	19097 / 0 / 905
Final R indices (I > 2$\sigma(I)$)[a]	R_1 = 0.10677 wR_2 = 0.1715
R indices (all data)	R_1 = 0.1447, wR_2 = 0.2043
GooF (all data)[b]	0.964
Max. peak/hole /e$^-$·Å^{-3}	4.17/-1.81

[a] $R_1 = \sum||F_o|-|F_c||/\sum|F_o|$; $wR_2 = \{\sum w[(F_o)^2-(F_c)^2]^2/\sum w[(F_o)^2]^2\}^{1/2}$

[b] GooF = $\{\sum w[(F_o)^2-(F_c)^2]^2/(n-p)\}^{1/2}$

3. ^{207}Pb NMR spectrum

The 207Pb NMR spectra were recorded on Bruker DRX500 Avance spectrometer operating at 104.5 MHz for a sample of 10 mM solution of single crystals in DMF. The 207Pb chemical shift was externally referenced to $Pb(NO_3)_2$ in D_2O (1M, 2961.2 ppm) at room temperature. The spectrum shows a single resonance at -785 ppm arising from the 12 chemically equivalent Pb atoms in the structure. The 207Pb NMR chemical shifts of $[Au@Pb_{12}]^{3-}$ are upfield relative to other known $[M@Pb_{12}]^{2-}$ ($[Pt@Pb_{12}]^{2-}$, +1780; $[Pd@Pb_{12}]^{2-}$, +1520; $[Ni@Pb_{12}]^{2-}$, +1167), which may be attributed to the different interstitial atom.

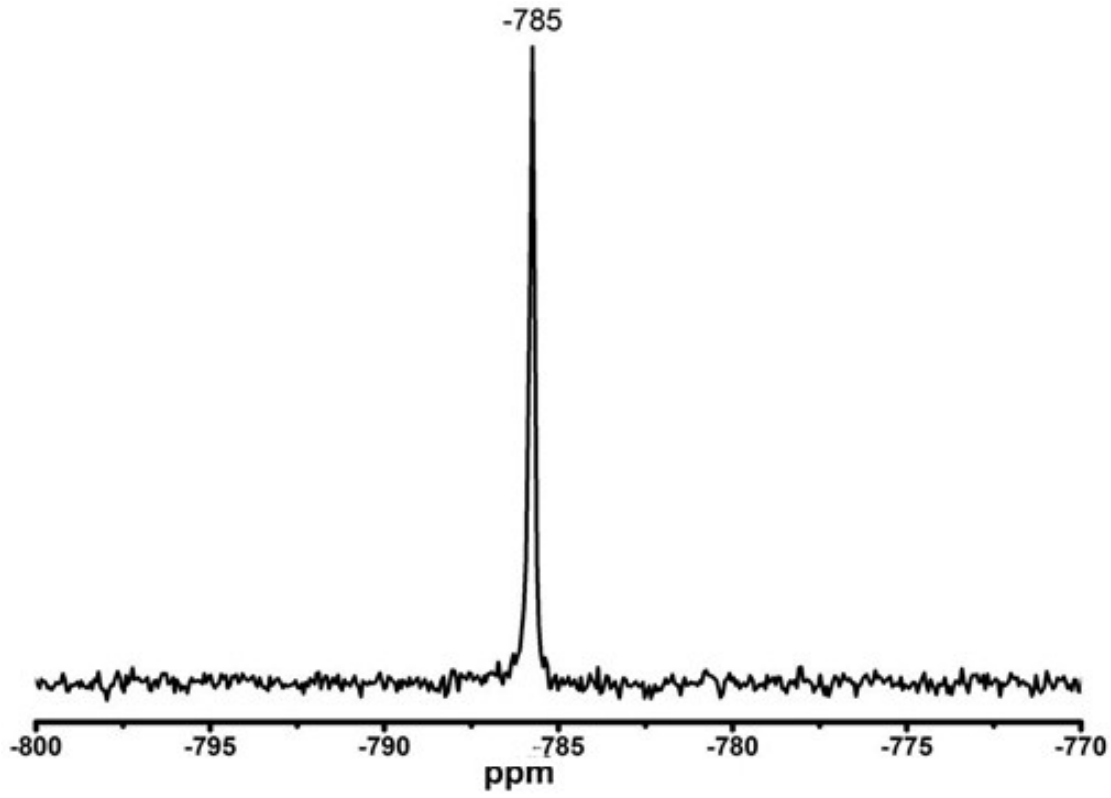

Figure S2: ^{207}Pb NMR spectrum of $[Au@Pb_{12}]^{3-}$ recorded in DMF at room temperature and 83.7 MHz.

4. Computational details

All the quantum chemical calculations were carried out using Gaussian 09 package[5]. The geometry optimization was performed using PBE0 functional[6-7] with Def2-TZVP basis set.[8] Compensation of the negative charges on the $[Au@Pb_{12}]^{3-}$ cluster was achieved by simulating mirror charges using the SMD model.[9] The natural population analysis (NPA)[10] was conducted based on the optimized structure using the NBO3.1 module as implemented in the Gaussian 09 package. The nucleus-independent chemical shifts (NICS) values[11] were computed with the Amsterdam Density Functional program (ADF 2013.01).[12-13] The scalar relativistic (SR) and spin−orbit coupling (SOC) effects were taken into account by the zero order regular approximation (ZORA). Valence triple-ζ plus one polarization (TZP) basis sets of Slater type were applied.

To understand the stability, both Pb_{12}^{2-} and Pb_{12}^{4-} were optimized at the PBE0/def2-TZVP level of theory. The Cartesian coordinates of the optimized structures and the energy levels of both Pb_{12}^{2-} and Pb_{12}^{4-} are given in Table S2 and Figure S3, respectively. Obviously, Pb_{12}^{2-} keeps the perfect icosahedral (I_h) symmetry, whereas, Pb_{12}^{4-} adopts a less compact prolate shape. Both anionic clusters have no imaginary frequency. The HOMO-LUMO gap of Pb_{12}^{4-} is much smaller than that of Pb_{12}^{2-} (1.90 eV *vs* 3.26 eV). As for Pb_{12}^{4-}, the extra two electrons fill the LUMO of Pb_{12}^{2-}, and this nearly introduced occupied orbital breaks the otherwise perfect I_h spherical symmetry of the cluster. In addition, the interactions between HOMO of Pb_{12} and 3d-orbital of Au have been plotted in Figure S4.

Chemical bonding analyses of $[Au@Pb_{12}]^{3-}$ was performed via the Adaptive Natural Density Partitioning method at the PBE0/Def2-TZVP level of theory. All the AdNDP calculations were performed using the Gaussian 09 software package and analyzed by the Multiwfn 3.3.9 software package.[14] In total, there are 62 valence electrons (31 pairs) in $[Au@Pb_{12}]^{3-}$ cluster. AdNDP transformed all these canonical molecular orbitals into the nc–2e bonding elements presented below (Figure S5).

Firstly, it found the following lone pairs (1c–2e) and classical (2c–2e) bonds:

1) Five d-type LPs on Au atom with ON=1.97-1.98 |e| (Figure S4a)
2) Twelve s-type LPs on each apical Pb atoms with ON=1.928 |e| (Figure S4b)
3) Four 4c-2e $AuPb_3$ σ bonds with ON=1.80-1.92 |e| (Figure S4c)
4) Six 12c-2e bonds with ON=2.00 |e| (Figure S4d)
5) Four 13c-2e π bonds with ON=2.00 |e| (Figure S4e)

It is note that four 13c-2e π bonds are formed by the interaction of 6p-orbitals of Pb with 6p-orbitals of Au. Essentially, these 8 π electrons satisfy the 2(N+1)2 rule with N=1, contributing to the strong stabilities of the cluster.

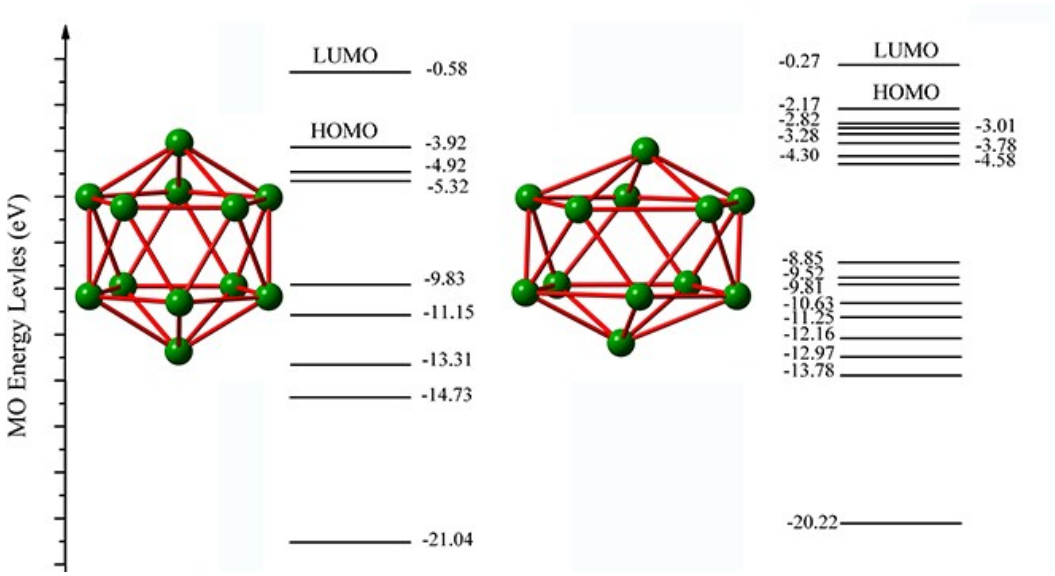

Figure S3. The molecular orbital energy levels of $[Pb_{12}]^{2-}$ (left) and $[Pb_{12}]^{4-}$ (right).

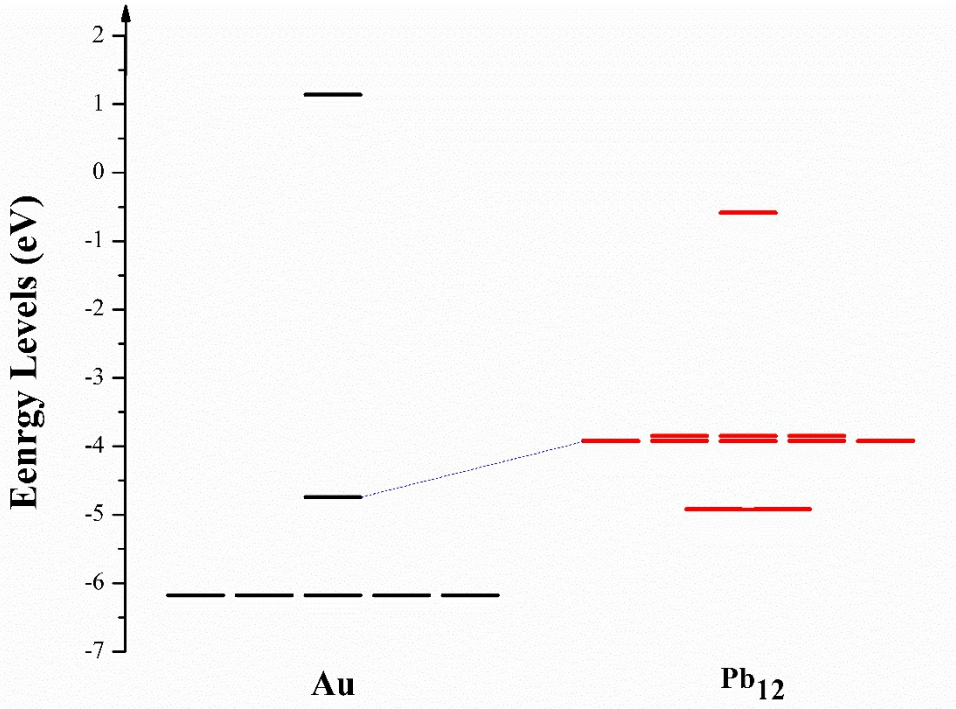

Figure S4. The interactions between HOMO of Pb_{12} and 3d-orbital of Au

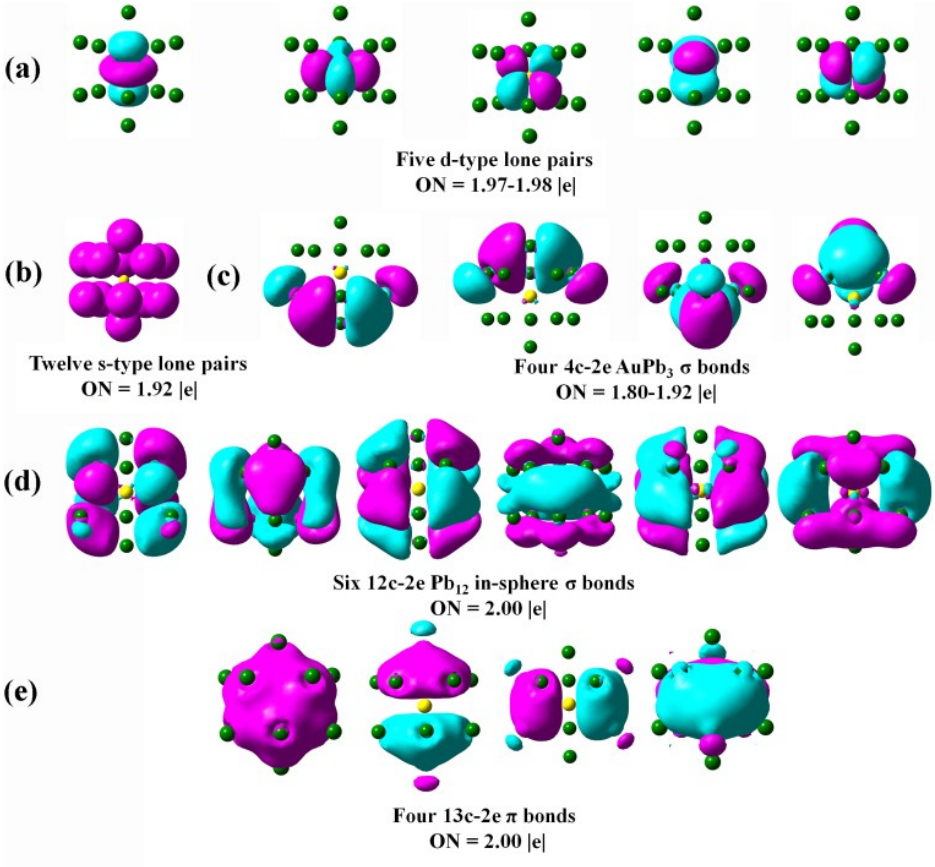

Figure S5 The AdNDP bonding pattern for $[Au@Pb_{12}]^{3-}$ grouped into five subsets with the corresponding occupation numbers (ON).

Table S2. Cartesian coordinates of the optimized structures of $[Au@Pb_{12}]^{3-}$, Pb_{12}^{2-} and Pb_{12}^{4-} at the PBE0/Def2-TZVP level of theory.

$[Au@Pb_{12}]^{3-}$	Pb	0.00000000	-2.19576838	2.37276826
	Pb	-2.69176227	-1.55408967	0.85454023
D_{3d}	Pb	1.90159120	-1.09788419	-2.37276826
	Pb	2.69176227	-1.55408967	0.85454023
	Pb	-1.90159120	-1.09788419	-2.37276826
	Pb	0.00000000	-3.10817934	-0.85454023
	Pb	-1.90159120	1.09788419	2.37276826
	Pb	1.90159120	1.09788419	2.37276826
	Pb	0.00000000	2.19576838	-2.37276826
	Pb	-2.69176227	1.55408967	-0.85454023
	Pb	2.69176227	1.55408967	-0.85454023
	Pb	0.00000000	3.10817934	0.85454023
	Au	0.00000000	-0.00000000	-0.00000000
Pb_{12}^{2-}	Pb	-0.00000000	-0.00000000	3.04990857
	Pb	-0.00000001	2.72792115	1.36396058
I_h	Pb	2.59440718	0.84297401	1.36396058
	Pb	1.60343184	-2.20693456	1.36396058

	Pb	2.59440719	-0.84297399	-1.36396058
	Pb	-1.60343181	-2.20693458	1.36396058
	Pb	-2.59440718	-0.84297401	-1.36396058
	Pb	1.60343181	2.20693458	-1.36396058
	Pb	-1.60343184	2.20693456	-1.36396058
	Pb	-2.59440719	0.84297399	1.36396058
	Pb	0.00000000	-0.00000000	-3.04990857
	Pb	0.00000001	-2.72792115	-1.36396058
Pb_{12}^{4-}	Pb	-0.19069836	0.26185869	3.42584636
	Pb	-0.20558151	2.90466567	1.83925724
C_i	Pb	2.29239125	0.86128319	1.41141199
	Pb	1.54510232	-2.13547532	1.02579321
	Pb	2.69931118	-1.09266264	-1.83583166
	Pb	-1.53413791	-1.91637077	1.41573122
	Pb	-2.29239125	-0.86128319	-1.41141199
	Pb	1.53413791	1.91637077	-1.41573122
	Pb	-1.54510232	2.13547532	-1.02579321
	Pb	-2.69931118	1.09266264	1.83583166
	Pb	0.19069836	-0.26185869	-3.42584636
	Pb	0.20558151	-2.90466567	-1.83925724

References

1. A. Spiekermann, S. D. Hoffmann, T. F. Fässler, *Angew. Chem. Int. Ed.* 2006, 45, 3459.
2. F. P. Gabbaï, S. C. Chung, A. Schier, S. Krüger, N. Rösch, H. Schmidbaur, 1997, *Inorg. Chem.* 36, 5699.
3. SMART and SAINT (software packages); Siemens Analytical X-ray Instruments, Inc., Madison, WI, 1996.
4. SHELXTL Program, version 5.1; Siemens Industrial Automation, Inc., Madison, WI, 1997.
5. M. J. Frisch, G. W. Trucks, H. B. Schlegel, G. E. Scuseria, M. A. Robb, J. R. Cheeseman, G. Scalmani, V. Barone, B. Mennucci, G. A. Petersson, H. Nakatsuji, M. Caricato, X. Li, H. P. Hratchian, A. F. Izmaylov, J. Bloino, G. Zheng, J. L. Sonnenberg, M. Hada, M. Ehara, K. Toyota, R. Fukuda, J. Hasegawa, M. Ishida, T. Nakajima, Y. Honda, O. Kitao, H. Nakai, T. Vreven, J. A. Montgomery Jr., J. E. Peralta, F. Ogliaro, M. Bearpark, J. J. Heyd, E. Brothers, K. N. Kudin, V. N. Staroverov, R. Kobayashi, J. Normand, K. Raghavachari, A. Rendell, J. C. Burant, S. S. Iyengar, J. Tomasi, M. Cossi, N. Rega, J. M. Millam, M. Klene, J. E. Knox, J. B. Cross, V. Bakken, C. Adamo, J. Jaramillo, R. Gomperts, R. E. Stratmann, O. Yazyev, A. J. Austin, R. Cammi, C. Pomelli, J. W. Ochterski, R. L. Martin, K. Morokuma, V. G. Zakrzewski, G. A. Voth, P. Salvador, J. J. Dannenberg, S. Dapprich, A. D. Daniels, Ö. Farkas, J. B. Foresman, J. V. Ortiz, J. Cioslowski and D. J. Fox, GAUSSIAN 09W (Revision A.1), Gaussian Inc., Wallingford, CT, 2010.
6. A. D. Becke, *Phys. Rev. A* 1988, 38, 3098.
7. J. P. Perdew, *Phys. Rev. B* 1986, 33, 8822.
8. A. Schaefer, H. Horn, R. Ahlrichs, *J. Chem. Phys.* 1992, 97, 2571.
9. a) S. Miertus, E.Scrocco; J. Tomasi, *Chem. Phys.* 1981, 55, 117; b) S.Miertus, *J.*Tomasi, *Chem. Phys.* 1982, 65, 239; c) M.Cossi, R.Barone, R.Cammi, *J.* Tomasi, *Chem. Phys. Lett.* 1996, 255,

327.

10. A. E. Reed, R. B. Weinstock, F. Weinhold, *J. Chem. Phys.* 1985, 83, 735.
11. P. v. R. Schleyer, C. Maerker, A. Dransfeld, H. Jiao, N. J. R. v. E. Hommes, *J. Am. Chem. Soc.* 1996, 118, 6317.
12. E. J. Baerends, et al. ADF, SCM, Theoretical Chemistry, Vrije Universiteit, Amsterdam, 2013. See http://www.scm.com.
13. J. P. Perdew, K. Burke, M. Ernzerhof, *Phys. Rev. Lett.* 1996, 77, 3865−3868.
14. T. Lu, F. W. Chen, *J. Comp. Chem.* 2012, 33, 580.